Polypropylene composites with natural carbon fillers obtained by rotational molding

Joanna Szymańska[1), *)] (ORCID ID: 0000-0002-9430-8676)**, Marek Szostak**[2)] (0000-0002-5822-3931)**, Dominik Paukszta**[1)] (0000-0001-8243-7035)

Abstract: PP composites with different contents of natural/waste carbon filler (1, 5, 10 and 25 wt.%) were obtained by rotational molding. Thermal properties (DSC), tensile properties and structure (optical and digital microscopy, WAXS) of PP composites were assessed. It was found that the composites are characterized by good surface quality of external walls and usually poorer quality of internal walls. The filler content affects both the degree of crystallinity and the mechanical properties of PP.

Keywords: polypropylene, carbonization, carbon fillers, composites, rotational molding.

Otrzymywanie kompozytów polipropylenowych z dodatkiem napełniaczy węglowych metodą formowania rotacyjnego

Streszczenie: Kompozyty PP o różnej zawartości naturalnego/odpadowego napełniacza węglowego (1, 5, 10 oraz 25% mas.) otrzymano metodą formowania rotacyjnego. Dokonano oceny właściwości termicznych (DSC), właściwości mechanicznych przy rozciąganiu i struktury (mikroskopia optyczna i cyfrowa, WAXS) kompozytów PP. Stwierdzono, że kompozyty charakteryzują się dobrą jakością powierzchni ścian zewnętrznych oraz zazwyczaj słabszą ścian wewnętrznych. Zawartość napełniacza ma wpływ zarówno na stopień krystaliczności, jak i na ich właściwości mechaniczne PP.

Słowa kluczowe: polipropylen, karbonizacja, napełniacze węglowe, kompozyty, formowanie rotacyjne.

Rotational molding is a polymer processing technique that enables the production of hollow plastic products in a wide range of sizes and shapes [1-3]. This method has been known since the mid-1940s, when the first polymer parts were successfully manufactured using this process [4]. The principle involves sintering polymer powder inside a rotating mold, which typically spins around two perpendicular axes. As the powder melts and adheres to the inner surface of the heated mold, it gradually forms a uniform layer that solidifies into a hollow product (Figure 1.).

The key advantages of roto molding include low production cost, simple and precise process control, and short lead times [5] which are processed for prolonged periods under temperature. The main process parameters studied are the shaft speed of the equipment, molding tem-
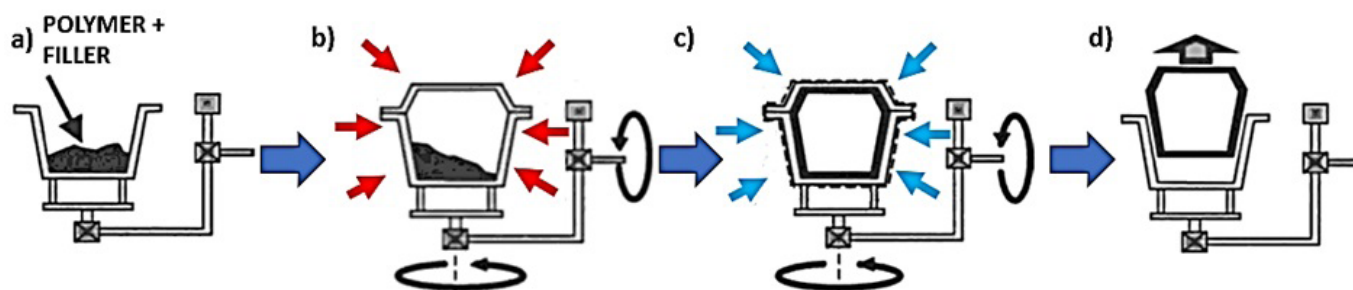

Fig. 1. The schematic process of rotational molding: a) placing polymer and filler in the mold, b) heating and rotating, c) cooling and rotating, d) demolding of the product [4]

[1)] Poznan University of Technology, Institute of Chemical Technology and Engineering, Faculty of Chemical Technology, ul. Berdychowo 4, 60-965 Poznań, Poland.

[2)] Poznan University of Technology, Institute of Materials Technology, Faculty of Mechanical Engineering, ul. Piotrowo 3, 60-965 Poznań, Poland.

*) Author for correspondence: joanna.szymanska@doctorate.put.poznan.pl

perature, polymer particle size, polymer melt flow index, and amount of material, which must be well controlled to achieve a non-degraded product with homogeneous thickness and no porosity. Rotomolded composites containing sisal, pine, coir, banana, flax, and maple wood fibers, among others, have been evaluated primarily for their mechanical (impact, flexural, and tensile strength. The process also offers excellent dimensional accuracy and surface finish, and it allows for adjustment of wall thickness without changing the mold design. Because the process operates under atmospheric pressure, the resulting parts are free from internal stresses, and material waste is minimal during manufacturing [1, 4, 6, 7].

Traditionally, roto molding has been used to produce large items such as tanks and containers. However, this technique requires polymers with high thermal stability due to long thermal cycles compared to other molding methods [8]. Therefore, the selection of polymer materials with low melting temperatures and good thermal resistance is crucial. Moreover, incorporating fillers into the polymer matrix is particularly challenging in roto molding due to its low-shear nature and lack of in situ mixing capabilities [9, 10].

In recent years, research has increasingly focused on developing polymer composites *via* rotational molding. Raymond and Rodrigue [11] successfully produced polyethylene–wood (maple) composites and examined the effects of filler (0–20 wt%) and blowing agent (0–0.6 wt%) on density, morphology, and mechanical properties. Their results showed that increasing wood content led to decreases in elongation at break and tensile strength, while tensile and flexural moduli improved, with the optimal filler content found at around 20 wt%. Lopez [12] studied the influence of fiber content and malleated polyethylene (MAPE) surface treatment on rotomolded composites reinforced with agave, coir, and pine fibers. Surface treatment significantly enhanced fiber–matrix compatibility for agave and coir, improving dispersion, reducing voids, and enhancing mechanical properties—particularly at fiber contents up to 30–40 wt%. However, at higher fiber contents, agglomeration and porosity led to decreased performance, highlighting the importance of fiber type and surface modification.

In the literature different polymer composites with another natural fillers are obtained by rotational molding e.g., banana and abaca fibres [6], wheat bran [13], black tea [14], cork [15], sisal, pine, coir, flax, and different wood fibers [5]. Despite growing interest, limited literature is available on the use of carbon-filled thermoplastic composites produced by roto molding. Nevertheless, this topic is starting to attract scientific attention. According to Ortega [10], around 13% of inorganic fillers used in polymer composites are carbon-based materials, such as carbon black, carbon fibers, and carbonates. The most used polymer matrices for rotomolded composites are polyethylene (PE), polyvinyl chloride (PVC), and polylactic acid (PLA). Polypropylene (PP) is less commonly used due to its high melting temperature, which makes standard injection-grade PP unsuitable for roto molding without specific modifications.

Some studies have explored the incorporation of carbon fillers such as graphite into PE matrices for roto molding, typically to improve fire retardancy and antistatic properties [16, 17]. Mhike and Focke [16] produced composites with up to 20 wt% graphite, while in a subsequent study [17] they used only 2 wt%. In both cases, mechanical properties decreased as filler content increased, suggesting a trade-off between functional and structural performance.

This study aims to develop carbon-filled polypropylene composites via rotational molding—a topic not yet thoroughly addressed in the available literature. The materials obtained are evaluated in terms of their structural and mechanical properties. The novelty of this research lies in the preparation of PP-based composites filled with low-cost, natural, waste-derived carbon fillers without prior melt mixing (e.g., extrusion), which could significantly reduce production costs. The main objective of this work is to investigate the effect of various carbon fillers on the thermal, mechanical, and structural properties of rotomolded PP composites.

EXPERIMENTAL PART

Materials

Polypropylene RMPP141 GREY 364 from the Australian company PSD ROTOWORX was used as the polymer matrix. This polymer in powder form (the dominant particle size 63–500 μm) is suitable for roto molding. The basic physical properties for this material are density of 0.900 g/cm^3 and melt flow rate (MFR) of 11 g/10min. Natural carbon materials were used as fillers. Two fractions of brown coal, xylite and leonardite, were selected, originating from the Sieniawa opencast mine in Poland [18]. The material particle sizes in 40–63 μm range. Tomato stalks (*Solanum lycopersicum L.*) were used after undergoing a carbonization process according to [19]. Carbonization process was conducted in a chamber reactor under an oxygen-free atmosphere, involving heating to 600°C at a rate of 3°C/min, followed by 1 hour isothermal stage. The resulting carbonizate was mechanically ground into particles with sizes in 40–63 μm range. Another filler used was coal dust, a waste byproduct from the refining process [20]. The coal dust was obtained from heavy oil fly ash (HOFA) and was washed to remove metal and sulfur compounds. It contains 50 to 80 wt% carbon, while the mineral content primally includes silicon, iron, aluminum, sulfur, and heavy metals—vanadium, nickel, molybdenum, or zinc. The material appears as a black or gray powder with low bulk density and consists of spherical, porous particles with a grain size in range of 10–120 μm (between 30–80 μm) and specific surface area above 6–15 m^2/g. All fillers were dried in a con-

T a b l e. 1. Roto molding process parameters

Parameter	Value
Mold speed – main axis, rpm	10
Mold speed – second axis, rpm	4
Furnace temperature, °C	240
Heating time, min	30
Cooling time, min	10
Mold dimensions, mm	61×61×185

vection dryer at 100°C for 24 hours. The incorporation of waste carbon fillers into a polymer matrix is a sustainable method of waste management aligned with circular economy principles. It also enables the production of composites at a significantly lower cost

Obtaining of composites

The selected carbons were crushed and separated into fractions on a sieve separator. A facies with a particle size of 40-63 µm was selected to obtain the composites. The filler was then dried at 80°C for 10 h. After weighing the appropriate amount of filler (1, 5, 10 and 25 g), it was added and mixed with polypropylene to obtain composites with filler (0, 1, 5, 10, 25 wt%).

The prepared premixes were sequentially placed in the mold and the rotational molding process started. The single-arm shuttle rotational molding machine produced by REMO GRAF, Poznan, was used to make samples. The set parameters are shown in Table 1. A summary of the samples obtained, together with the determinations used in the work, is summarized in Table 2.

The samples were obtained in the form of hollow cuboids (Figure 2). As the filler addition increased, the color and surface texture of the sample changed, what can be seen on Figure 2, where the PP/xylite composites samples are shown.

It was not possible to obtain PP_O_25 and PP_T_25 composites (Table 2). For such a big number of fillers the agglomeration of the filler around the polymer particles was observed for PP filled with 25 wt% of carbonized

T a b l e 2. Description of the samples analyzed

Sample	Filler, wt%
PP	Control sample, 0
PP_C_1	Xylite (brown carbon), 1
PP_C_5	Xylite, 5
PP_C_10	Xylite, 10
PP_C_25	Xylite, 25
PP_L_1	Leonardite (brown carbon), 1
PP_L_5	Leonardite, 5
PP_L_10	Leonardite, 10
PP_L_25	Leonardite, 25
PP_O_1	Waste dust from the refining industry, 1
PP_O_5	Waste dust from the refining industry, 5
PP_O_10	Waste dust from the refining industry, 10
PP_O_25	Waste dust from the refining industry, 25 – NO samples obtained
PP_T_1	Carbonized tomato stems, 1
PP_T_5	Carbonized tomato stems, 5
PP_T_10	Carbonized tomato stems, 10
PP_T_25	Carbonized tomato stems, 25 – NO samples obtained

tomato stems (Figure 3). It blocked the heat flow, and the polymer did not melt in the mold.
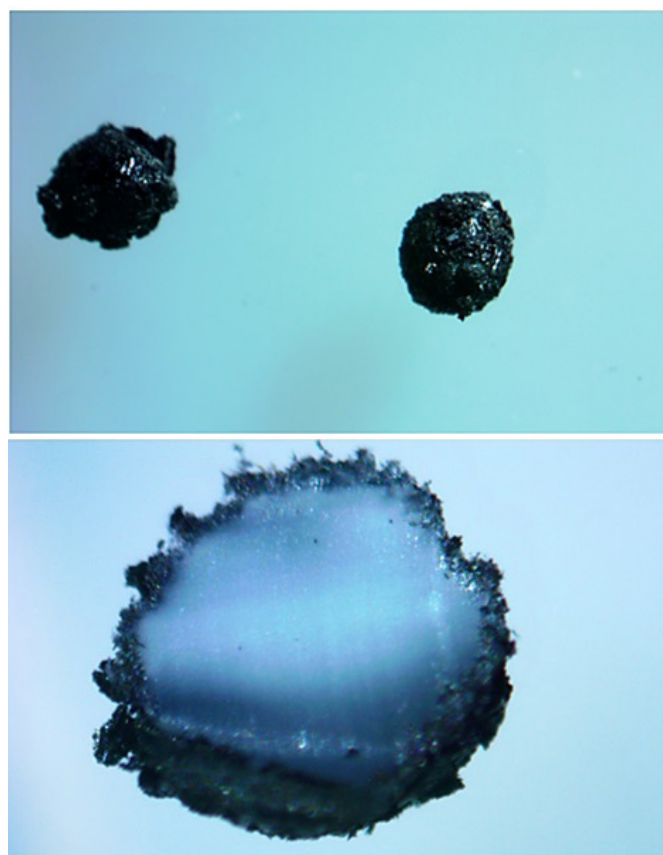

Fig. 3. Microscopic images of a polymer granule surrounded by the carbonized tomato stems (on the top), cross-section of the granule with a visible carbon coating (on the bottom)

Fig. 2. Images of composites after rotational molding (from the left PP, then PP/xylite composites with different filler content)

Methods

Wide angle X-ray scattering

Wide angle X-ray scattering (WAXS) structural analysis was performed on the fillers, polymer matrix and composites. The horizontal diffractometer TUR M-62 (Germany), CuKα radiation, at 30 kV and 20 mA anode excitation, with an HZG-3 goniometer was used. All the diffractograms were recorded in a range of 2Θ between 10–30° with a step of 0.04° (Cu K$_\alpha$ radiation, after Ni filtration).

The next step was the numerical analysis of the diffractograms. This calculation method is based on the work of Hindeleh and Johnson [21] (modified by Rabiej [22]). The degree of crystallinity (X_c) was calculated using the formula (Equation 1).

$$X_c = \frac{P_c}{P_c + P_a} \qquad (1)$$

where: P_a – the area of the amorphous peak, P_c – the sum of the areas of crystalline peaks.

The areas were determined by using a graphical method by separating the peaks, applying deconvolution, and integrating the functions. The following seven diffraction peaks were used to calculate X_c: (110), (040), (130), (111), (131) and (041) from the α-form and (300) from the β-form.

Differential scanning calorimetry

Samples were characterized using differential scanning calorimetry (DSC) with Netzsch DSC 200, manufactured in Germany. The 8 mg samples were prepared and placed in the measuring cup. Heated to 200°C (rate 10°C/min) under nitrogen. To remove thermal history, samples were kept at this temperature for 5 min. The samples were cooled from 200°C to 40°C (rate 5°C/min) and then reheated. The second cycle was analyzed. The crystallization temperature (T_c) was obtained from the exothermic peak and the melting temperatures (T_m) from the endothermic peaks. The half-time crystallization and the transformation curve were also determined.

Mechanical properties

A Zwick Roell Z020 (Ulm, Germany) mechanical testing machine was used to determine the mechanical properties of the specimens. The test was performed under parameters: the load cell capacity was 20 kN at a crosshead speed of 5 mm/min. All mechanical properties of the composites were obtained in accordance with the EN-PN ISO 527 specification. For each material, eight specimens were evaluated, and the average was calculated.

Optical microscopy

Microscopic images of the samples were taken using a light microscope (OPTIKA Microscopes, Italy). The microscope was equipped with a TOUPCAM optical camera. Photographs were taken of a polymer granule surrounded by the carbonized tomato stems.

Digital microscopy

The images of the internal surface of the samples were taken on the KEYENCE VHX-7000 high-definition 4K Digital Microscope (Belgium) with the 50× magnification.

RESULTS AND DISCUSSION

Structural characterization

The WAXS analysis was performed to investigate the effect of carbon fillers and rotational molding process on the supermolecular structure of the polypropylene matrix. Considering the results presented in Table 3, the largest share of the crystalline phase in the samples occurs in PP without filling (54%). For all carbon types, X_c is lower than for the control sample. There is also a tendency that with the increase of filler concentration there is a proportional decrease of X_c. This may be due to the addition of carbon fillers, which are not active nucleates [18]. During the rotational molding process, there are also no shear forces that affect the crystallinity of the samples [23, 24].

The crystallization process of the polymer can be destabilized by the addition of carbon fillers. Due to this fact, the decrease in the degree of crystallinity has been observed. This can be related to the reduction of the mobility of the iPP chains. These observations agree with reports by Le Digabel [25] and Girones [26].

T a b l e 3. Degree of crystallinity for PP and composites

Sample	X_c, %
PP	54.0
PP_C_1	45.5
PP_C_5	42.9
PP_C_10	41.7
PP_C_25	36.0
PP_L_1	49.1
PP_L_5	47.7
PP_L_10	42.7
PP_L_25	36.9
PP_O_1	49.7
PP_O_5	48.0
PP_O_10	46.3
PP_O_25	-
PP_T_1	52.2
PP_T_5	52.3
PP_T_10	50.7
PP_T_25	-

T a b l e 4. Thermal characterization of PP and composites

Sample	T_m, °C	T_c, °C	$t_{0.5}$, s
PP	165.2	129.7	71
PP_C_1	164.8	129.8	101
PP_C_5	165.1	129.6	81
PP_C_10	165.6	129.0	78
PP_C_25	165.5	129.0	84
PP_L_1	165.3	129.8	87
PP_L_5	164.8	129.5	88
PP_L_10	164.5	129.5	90
PP_L_25	164.4	128.2	128
PP_O_1	164.4	130.0	85
PP_O_5	165.6	129.4	91
PP_O_10	165.1	129.2	103
PP_O_25	–	–	–
PP_T_1	165.2	130.1	85
PP_T_5	165.9	130.0	79
PP_T_10	166.6	128.7	84
PP_T_25	–	–	–

Thermal characterization

The thermal properties of the composites such as crystallization temperature (T_c), melting temperature (T_m) and half time of crystallization are presented in Table 4. The data presented are from the second heating/cooling cycles. The T_m of all samples is stable in the range from 164°C to 167°C. It indicates that the incorporation of carbon fillers had a limited impact on the melting behavior of the PP matrix. The highest T_m was recorded for the PP_T_10 sample (166.6°C). The T_c were also relatively unaffected by filler addition, with most values around 129–130°C. The results obtained confirm previous WAXS analysis data and the non-significant effect of carbon fillers on the nucleation and crystallization process of PP matrix.

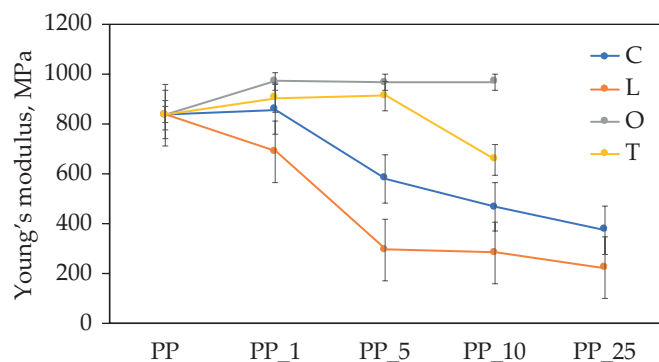The kinetic of crystallization expressed as half-time of crystallization ($t_{0.5}$) is more affected by filler type and content. Pure PP showed the shortest crystallization time equal to 71 s. The addition of carbon fillers in general led to slower crystallization processes. It may be also connected with the reduction of the mobility of the PP chains. The most significant decrease of $t_{0.5}$ was observed for PP_L_25 (128 s). Some of the samples has similar value as control sample, for example PP_C_10 – 78 sand PP_T_5 – 79 s.

Mechanical properties

The mechanical properties of PP and composites are shown in Figures 4–6. It is clear from Figure 4 that Young's modulus for PP_O composites is higher than for other composites and control samples and is also stable for any amount of filler. Also, in the case of PP_T composites with a filler content of 1 and 5 wt%, the Young's modulus is higher than that of PP but increasing the filler content to 10 wt% causes its decrease. In the case of PP_C composites, adding 1% of filler does not affect the modulus, but increasing the amount of filler reduces the Young's modulus. The lowest Young's moduli are observed in the case of PP_L composites for all filler concentrations. The poor adhesion between the filler particles and the polymer matrix may be responsible for this effect.

The tensile strength of composites is lower compared to PP, as illustrated in Figure 5. The lowest tensile strength was observed for composites filled with leonardite for all filler concentrations. On the other hand, the highest was observed for PP_O composites. For all composites, there is a tendency for the tensile strength to decrease with increasing filler content.

The elongation at break decreases with increasing filler content (Fig. 6). All composites show the same elongation at break at the lowest filler content (1 wt%).

Tensile properties of composites are consistent with the available literature data. In most cases, the mechanical properties decrease when the filler is added in the roto molding process. Barczewski *et al.* [9] also noted a decrease in tensile properties (tensile strength, tensile modulus, elongation at break) in composites with 5 wt%
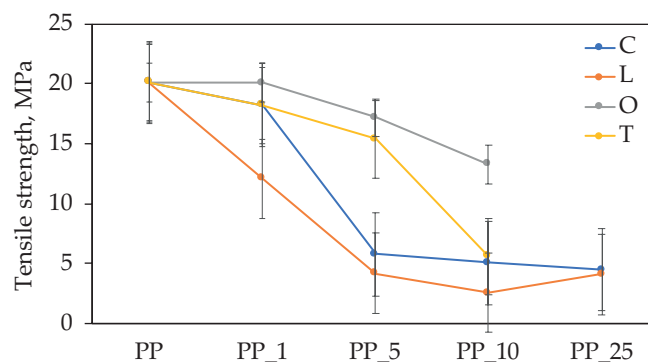

Fig. 4. Young's modulus of composites (C – xylite, L – leonardite, O – waste dust from the refining industry, T – carbonized tomato stems)

Fig. 5. Tensile strength of composites (C – xylite, L – leonardite, O – waste dust from the refining industry, T – carbonized tomato stems)
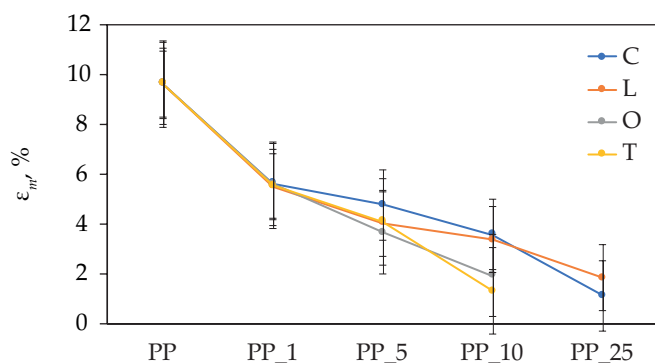
Fig. 6. Elongation at break of composites (C – xylite, L – leonardite, O – waste dust from the refining industry, T – carbonized tomato stems)

filler content. The filler modification does not help to obtain the composite with higher properties than the control sample. Dou [27] added small amount of the filler (0.1–0.5%) to the polymer matrix and all obtained composites had lower all mechanical properties. Anisko *et al.* [28] showed a decrease in some mechanical properties and defects in the structure. Computed tomography and density measurements showed that porosity was closely related to the size and shape of the polymer particles, with irregular shapes and large particles leading to more defects. FT-IR and colorimetric analysis confirmed the degradation effects in samples processed without heat pretreatment. The study also showed that pretreated PLA powders had more uniform wall thickness and better surface.

In this work, the reduced mechanical properties are also due to the porous structure of the composites. To verify and confirm this hypothesis, microscopic analyses were performed.

Digital microscopy

Figures 7a–e presents the structure of the inner surface of the obtained rotomolded samples are shown.

Above, the digital microscope photos show the structure of one selected internal surface of the obtained walls of rotomolded castings from original PP, and it composites with natural carbon fillers. In addition to the smooth and uniform internal surface for samples made of original polypropylene, for all composites samples produced, it was observed that the surface is more rough and uneven, and with a higher content of carbon filler (5 wt% and more), holes also appear after air bubbles diffusing from the inside of the samples materials into the volume of the mold. It can also be observed that the carbon filler is mostly located between the grains of polypropylene powder, which is especially visible for low filler contents (1 wt%).

The best internal surface is characterized by samples made of PP_O; then PP_L and PP_C. In the case of samples produced from PP and 1% carbonized tomato composites, the internal surface of the product is smooth, but for 5%

of this filler content, holes and quite deep craters appear on it. For PP composites containing 10% of various carbon fillers, the fillers accumulate on the inner surface of the samples, which is particularly visible for PP_T composite.

However, as shown in Figure 7e–g, the quality of the external surface of the samples is at least good and allows obtaining good strength and aesthetic rotomolded products as a result.

Holes, porosity, and lack of homogeneity are also frequently mentioned in other works as characteristics of materials obtained by this method. Robledo-Ortíz [29] highlighted the resulting holes and defects and the incompatibility of the filler with the matrix. He studied composites of polyethylene reinforced with natural fibers (agave and coconut) processed by rotational molding. To improve the structure of the composites and increase the compatibility of the fibers with the matrix, the fibers were surface treated with maleated polyethylene (MAPE). Composites with untreated fibers showed poor dispersion and high porosity, while MAPE-treated fibers resulted in better interfacial adhesion, more uniform morphology, and reduced voids.

Pethrick and Hudson [3] proposed a simplified theoretical framework to enhance the understanding of the complex process of rotational molding. Authors divided the process into three main stages: powder deposition and melting, bubble removal and consolidation, and finally, cooling and solidification. Viscosity played a critical role throughout, influencing powder fusion, bubble evacuation, and the uniformity of the final wall thickness. While low melt viscosity facilitates bubble removal, it may compromise wall stability –particularly in thick-walled parts. The study highlights the importance of carefully controlled heating and cooling cycles, as these directly affect crystal structure development and, consequently, mechanical properties. The authors also observe that increasing the intensity of the heating step can promote more efficient bubble removal, resulting in a smoother and more homogeneous surface. However, prolonged thermal exposure may lead to oxidative degradation or, in some cases, increased viscosity due to physical transformations, degrading the composite's mechanical performance. Crawford also discussed this phenomenon [30, 31]. As such, precise design and control of the process temperature profile are essential to ensuring optimal product quality [32].

CONCLUSIONS

The research presented in this study focuses on the development of polypropylene–natural carbon composites using the rotational molding technique. Subsequently, the properties of the composites obtained were thoroughly analyzed. As a result of the research, it was possible to obtain samples from the manufactured PP composites with natural carbon fillers with good external wall surfaces and most often with poor internal walls. The best

a)

b)

c)

d)

e)

f)
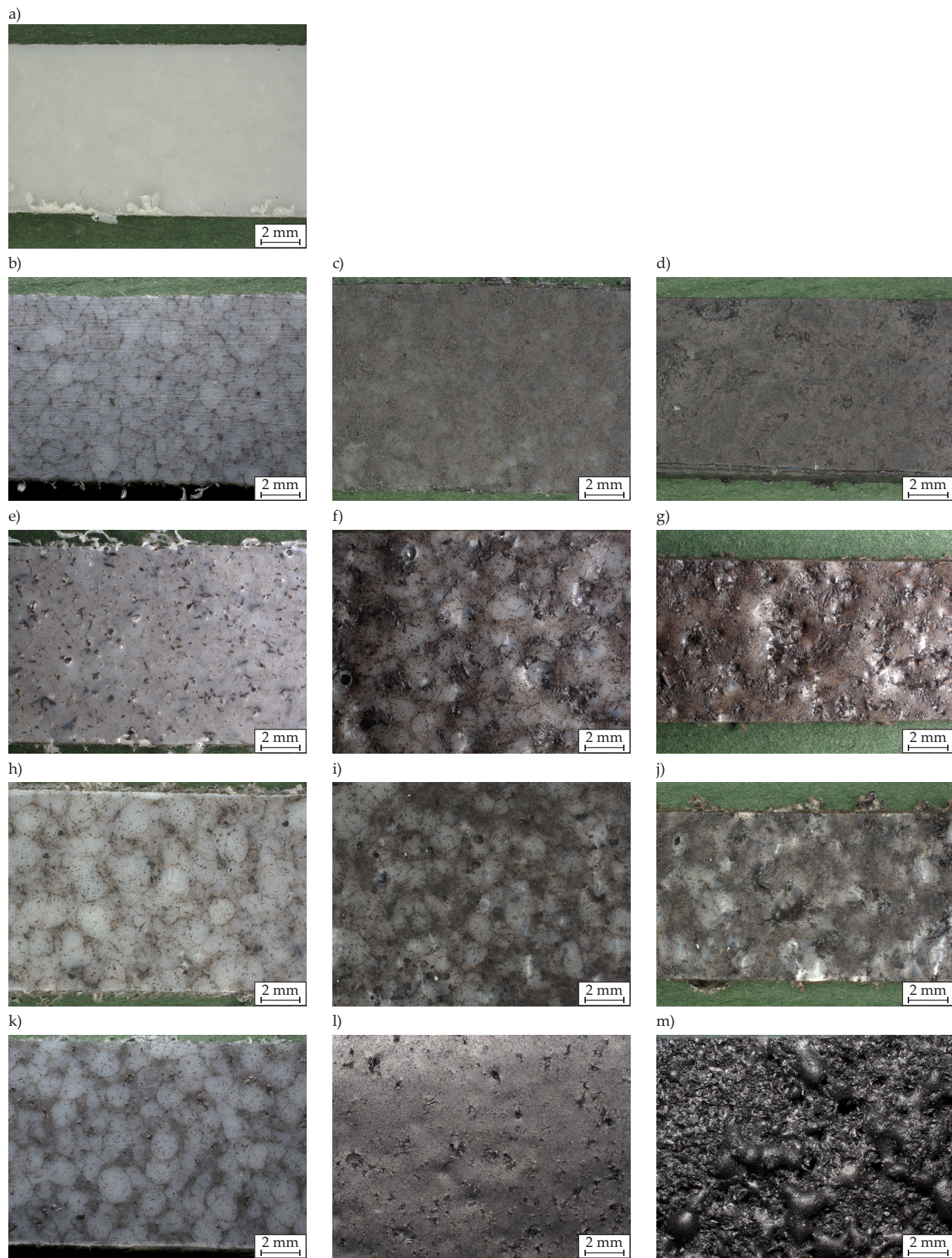

g)

h)

i)

j)

k)

l)

m)

Fig. 7. Microscopy images: a) PP, b) PP_O_1, c) PP_O_5, d) PP_O_10, e) PP_C_1, f) PP_C_5, g) PP_C_10, h) PP_L_1, i) PP_L_5, j) PP_L_10, k) PP_T_1, l) PP_T_5, m) PP_T_10; magnification 50´.

mechanical properties were obtained for characterized by the rotomolded samples made of PP composites with the addition of waste dust from the refining industry, then PP composites with carbonized tomato stems. For this composite, with the increase in the filler content to 5 wt%, an increase in Young's modulus and elongation at break was observed. For extremely high carbon filler contents (25 wt%), it surrounds the surface of PP powder grains. The degree of crystallinity of the manufactured rotomolded composites decreases with the increase in the carbon filler content. The content of carbon fillers in the composites does not affect the softening temperature and crystallization temperature. Only the half-time crystallization is always higher compared to PP matrix. Research has shown that it is possible to obtain good quality rotomolded products from PP composites and natural carbon fillers, especially for waste dust filler from the refining industry.

Authors contribution

J.Sz. – conceptualization, methodology, investigation, writing-original draft, writing-review and editing; M.S. – conceptualization, methodology, writing-original draft; D.P. – conceptualization, supervision.

Conflict of interest

The authors declare no conflict of interest.

REFERENCES

[1] Oliveira M.J., Cramez M.C.: *Journal of Macromolecular Science, Part B* **2001**, *40(3-4)*, 457.
https://doi.org/10.1081/MB-100106170

[2] Crawford R.J.: *Journal of Materials Processing Technology* **1996**, *56(1-4)*, 263.
https://doi.org/10.1016/0924-0136(95)01840-9

[3] Pethrick R.A., Hudson N.E.: *Proceedings of the Institution of Mechanical Engineers, Part L: Journal of Materials: Design and Applications* **2008**, *222(3)*, 151.
https://doi.org/10.1243/14644207JMDA123

[4] Crawford R.J., Throne J.L.: "Rotational molding technology", William Andrew Publishing, New York 2002.

[5] León L.D.V.E., Escocio V.A., Visconte L.L.Y. *et al.*: *Journal of Reinforced Plastics and Composites* **2020**, *39(11-12)*, 459.
https://doi.org/10.1177/0731684420916529

[6] Ortega Z., Monzón M.D., Benítez A.N. *et al.*: *Materials and Manufacturing Processes* **2013**, *28*, 879.
https://doi.org/10.1080/10426914.2013.792431

[7] López-Bañuelos R.H., Moscoso F.J., Ortega-Gudiño P. *et al.*: *Polymer Engineering and Science* **2012**, *52(12)*, 2489.
https://doi.org/10.1002/pen.23168

[8] Tcharkhtchi A., Perrot E., Chinesta F.: *International Polymer Processing* **2004**, *19(3)*, 296.
https://doi.org/10.3139/217.1835

[9] Barczewski M., Szostak M., Nowak D. *et al.*: *Polimery* **2018**, *63(11-12)*, 772.
https://doi.org/10.14314/polimery.2018.11.5

[10] Ortega Z., McCourt M., Romero F. *et al.*: *Polymers* **2022**, *14(23)*, 5260.
https://doi.org/10.3390/polym14235260

[11] Raymond A., Rodrigue D.: *Cellular Polymers* **2013**, *32(4)*, 199.
https://doi.org/10.1177/026248931303200401

[12] Cisneros-López E.O., González-López M.E., Pérez-Fonseca A.A. *et al.*: *Composite Interfaces* **2017**, *24*, 35.
https://doi.org/10.1080/09276440.2016.1184556

[13] Hejna A., Barczewski M., Andrzejewski J. *et al.*: *Polymers* **2020**, *12(5)*, 1004.
https://doi.org/10.3390/polym12051004

[14] Barczewski M., Ortega Z., Piaskowski P. *et al.*: *Composites Part C: Open Access* **2024**, *13*, 100437.
https://doi.org/10.1016/j.jcomc.2024.100437

[15] Martins C.I., Gil V.: *Frontiers in Materials* **2020**, *7*, 297.
https://doi.org/10.3389/fmats.2020.00297

[16] Mhike W., Focke W.W.: *Journal of Vinyl and Additive Technology* **2013**, *19(4)*, 258.
https://doi.org/10.1002/vnl.21316

[17] Mhike W., Focke W.W., Asante J.L.: *Journal of Thermoplastic Composite Materials* **2017**, *31(4)*, 535.
https://doi.org/10.1177/0892705717712634

[18] Szymańska J., Bednarek W.H., Szostak M. *et al.*: *Journal of Natural Fibers* **2023**, *20*, 2190553.
https://doi.org/10.1080/15440478.2023.2190553

[19] Szymańska J., Doczekalska B., Strzemiecka B. *et al.*: *Journal of Natural Fibers* **2023**, *20(2)*, 2282047.
https://doi.org/10.1080/15440478.2023.2282047

[20] Szymanska J., Bednarek W.H., Urbaniak W. *et al.*: "Polypropylene composites with waste carbon material from the petrochemical industry," article in-press, **2025**.

[21] A. M. Hindelehy and D. J. Johnson, "The resolution of multipeak data in fibre science".

[22] Rabiej M.: *Journal of Applied Crystallography* **2014**, *47*, 1502.

https://doi.org/10.1107/S1600576714014782

[23] Jay F., Haudin J.M., Monasse B.: *Journal of Materials Science* **1999**, *34*, 2089.
https://doi.org/10.1023/A:1004563827491

[24] Varga J., Karger-Kocsis J.: *Journal of Polymer Science Part B: Polymer Physics* **1996**, *34(4)*, 657.
https://doi.org/10.1002/(SICI)1099-0488(199603)34:4<657: AID-POLB6>3.0.CO;2-N

[25] Le Digabel F., Boquillon N., Dole P. *et al.*: *Journal of Applied Polymer Science* **2004**, *93(1)*, 428.
https://doi.org/10.1002/app.20426

[26] Girones J., Vo L.T.T., Haudin J.M. *et al.*: *Polymer* **2017**, *127*, 220.

[27] Dou Y., Rodrigue D.: *Cellular Polymers* **2021**, *40(5)*, 198.
https://doi.org/10.1177/02624893211018825

[28] Aniśko J., Barczewski M., Mietliński P. *et al.*: *Polymer Testing* **2022**, *107*, 107481.
https://doi.org/10.1016/j.polymertesting.2022.107481

[29] Robledo-Ortíz J.R., González-López M.E., Rodrigue D. *et al.*: *Journal of Polymers and the Environment* **2020**, *28*, 1040.
https://doi.org/10.1007/s10924-020-01667-1

[30] Spence A.G., Crawford R.J.: *Proceedings of the Institution of Mechanical Engineers, Part B: Journal of Engineering Manufacture* **1996**, *210(6)*, 521.
https://doi.org/10.1243/PIME_PROC_1996_210_151_02

[31] Xu L., Crawford R.J.: *Journal of Materials Science* **1993**, *28*, 2067.
https://doi.org/10.1007/BF00367563

[32] Cramez M.C., Oliveira M.J., Crawford R.J.: *Proceedings of the Institution of Mechanical Engineers, Part B: Journal of Engineering Manufacture* **2003**, *217(3)*, 323.
https://doi.org/10.1243/095440503321590497